

Original Article

CCR6⁺ B lymphocytes responding to tumor cell-derived CCL20 support hepatocellular carcinoma progression via enhancing angiogenesis

Huan He^{1,4*}, Jianxiong Wu^{2*}, Mengya Zang^{1*}, Weihu Wang^{5,6*}, Xiuli Chang¹, Xiangmei Chen³, Ruijun Wang¹, Zhiyuan Wu^{1,4}, Liming Wang², Dongmei Wang^{1,4}, Fengmin Lu³, Zongtang Sun⁴, Chunfeng Qu^{1,4}

Departments of ¹Immunology, ²Abdominal Surgery, National Cancer Center/Cancer Hospital, Chinese Academy of Medical Sciences and Peking Union Medical College, Beijing 100021, P. R. China; ³Department of Microbiology & Infectious Disease Center, School of Basic Medical Science, Peking University Health Science Center, Beijing 100191, P. R. China; ⁴State Key Lab of Molecular Oncology, National Cancer Center/Cancer Hospital, Chinese Academy of Medical Sciences and Peking Union Medical College, Beijing 100021, P. R. China; ⁵Department of Radiotherapy, National Cancer Center/Cancer Hospital, Chinese Academy of Medical Sciences and Peking Union Medical College, Beijing 100021, P. R. China. ⁶Currently Address: Key Laboratory of Carcinogenesis and Translational Research (Ministry of Education/Beijing), Department of Radiation Oncology, Peking University Cancer Hospital & Institute, Beijing 100142, P. R. China. *Equal contributors.

Received October 20, 2016; Accepted March 2, 2017; Epub May 1, 2017; Published May 15, 2017

Abstract: Background & Aims: Different immune cells in tumor microenvironment shape tumor progression. CCL20 over-expression was reported as one of the “stemness” trait in TP53 mutated hepatocellular carcinoma (HCC). We aimed to understand the effect of CCL20 on HCC progression. Methods: In two HCC cohort patients (n=95, n=85 respectively), serum CCL20 concentration was quantified by using ELISA. Expressions of CCL20 and CCR6 in 41 paired HCC tumor and adjacent non-tumor tissues were determined by quantitative Real-Time PCR, confirmed by immunohistochemistry (CCL20) or by flow cytometry analysis (CCR6). Chemotaxis of splenocytes or purified CD19⁺ B cells to tumor cell-derived CCL20, and angiogenesis of different CD19⁺ B subtypes responding to tumor cell-derived CCL20 were measured *in vitro*. H22 murine hepatoma cells were inoculated into immunocompetent or immunodeficient SCID mice, tumor growth and metastasis were monitored after the mice were treated with anti-CCL20 neutralizing antibody or depleted B cells by anti-CD20. Results: Elevation of pretherapy serum CCL20 in HCC patients and increase of CCR6 expression in HCC tissues were closely associated with tumor metastasis and disease poor prognosis. In HCC tissues, CCL20 expression was positively correlated with CCR6 ($R^2=0.3134$, $P=0.0002$), and CCR6 was exclusively identified in tumor infiltrated immune cells. CD19⁺CD5⁺ B lymphocytes expressed higher CCR6, responded to tumor cell-derived CCL20 and enhanced angiogenesis *in vitro*. Neutralizing CCL20 activity in immunocompetent mice, not in SCID mice, attenuated tumor incidence, restrained tumor growth and distal metastasis. Tumor angiogenesis was significantly inhibited after CCL20 activity was blockade. In addition, inhibiting B lymphocyte infiltration into tumor mileum also attenuated tumor growth. Conclusions: Tumor cell-derived CCL20 interacts with CCR6 highly expressed CD19⁺CD5⁺ B cells, to promote HCC progression, which might be via enhancing angiogenesis.

Keywords: B lymphocytes, CCL20, CCR6, microenvironment, hepatocellular carcinoma

Introduction

Hepatocellular carcinoma (HCC) is one of the most common cancers with a poor outcome as lack of treatment options. Currently, hepatic resection is still the mainstay of curative treatment for HCC which is confined to the liver with satisfactory liver function [1]. However, recurrence rate can be as high as 80% of Asian patients within 5 years after resection [2].

Several prediction models for recurrence risk assessment based on the tumor gene signatures have been developed. In the latest decade several studies demonstrated that the gene signatures both from HCC tumorous tissues and from tumor-adjacent tissues were significantly associated with the patients' progression [3, 4]. Among them, the gene signatures in the tumor microenvironment related to immune responses and inflammation were found mostly related

to the disease progression [5, 6]. Chemokines are critical both in physiological and inflammatory conditions to direct the mobilization of leukocytes via interacting with their related chemokine receptors expressed on different cell types [7]. CCL20, named as liver and activation-regulated chemokine (LARC), or macrophage inflammatory protein-3 α (MIP-3 α), or Exodus-1 previously, is one of the CC chemokines expressed in several tissues and different cell types. In HCC, CCL20 over-expression was reported as one of the “stemness” trait in TP53 mutated HCC [8]. Some studies reported that CCL20 could promote the HCC cell proliferation and migration by inducing epithelial-mesenchymal transition-like changes via PI3K/PKB and Wnt/ β -catenin pathways [9]. In addition to the direct effect of CCL20 on the tumor cells, very recent study reported that HCC mesenchymal cell-derived CCL20 induced the monocyte-derived macrophages to express indoleamine 2,3-dioxygenase (IDO), which supported HCC progression via establishing an immunosuppressive tumor microenvironment [10]. Therefore, the HCC progression could be influenced significantly by the infiltrated immune cells in response to HCC-derived CCL20.

In the tumor microenvironment there were a large amount of heterogeneous immune cells that displayed different effects to shaped the tumor growth and diseases progression [11]. CCR6 is the sole selective chemokine receptor for CCL20. The interaction of CCL20 and CCR6 gave rise to different biological consequences in homeostasis and pathology as the involvement of distinct CCR6-expressing cells, including immature dendritic cells, effector/memory T cells, B cells, and NK cells [12]. In addition to the tumor-associated macrophages, the effects of B lymphocytes on tumor development had been documented recently [13-15]. The effect of blocking CCL20 activity on HCC growth and metastasis *in vivo* is still unknown. In the current study, we found that HCC cells-derived CCL20 could promote HCC progression via recruiting CCR6-expressed B lymphocytes, especially the CD19⁺CD5⁺ B cells. Blockade of CCL20 activity restrained the HCC growth and metastasis in the immunocompetent mice. Elevated pretherapy serum CCL20 in HCC patients might be a potential target for HCC relapse intervention.

Materials and methods

Ethics statement

All samples were collected with informed consent from patients, and all related procedures were performed with the approval of the Institutional Ethics Committee of Cancer Hospital, Chinese Academy of Medical Sciences in Beijing (CH-CAMS, CH-BMS-002). All procedures involving mice were approved by the Institutional Animal Care and Use Committee at CH-CAMS (NCC2014A011).

Patients and specimens

Two HCC cohort of 180 patients from CH-CAMS (n=95) and Henan Provincial Cancer Hospital (n=85) as described previously were included in the study [16, 17]. Their pretherapy serum samples were stored in -80°C and the patients with lung metastasis or intrahepatic recurrence with vascular invasion were defined as HCC metastasis. In addition, 6 cases of normal hepatic tissues were obtained from Beijing YouAn Hospital, Capital Medical University.

Mice and cell lines

C57BL/6 mice, Balb/C mice and severe combined immune deficiency (SCID) mice were all purchased from Beijing HFK Bioscience, Chinese Academy of Sciences. Human HCC cell lines MHCC97L and MHCC97H were generously provided by Dr. Ran (Chinese Academy of Medical Sciences, Beijing); HepG2, Hep3B and mouse hepatoma cell line Hepa1-6 were purchased from ATCC, USA. HCC cell line Huh7, 7703, mouse hepatoma H22 cell line and human umbilical vein endothelial cells (HUVEC) were purchased from Type Culture Collection of Chinese Academy of Science, Shanghai, China. Cells were cultured in Dulbecco's Modified Eagle's Medium (DMEM) or RPMI-1640 medium supplemented with 10% fetal bovine serum (Hyclone).

Determination of CCL20 expression and production

Serum levels of CCL20 in HCC patients and the concentrations in cell supernatant were measured using ELISA kits purchased from Wuhan USCN, China, according to the manufacturer's instructions. CCL20 transcriptional levels were

CCR6⁺ B lymphocytes recruited by tumor-secreted CCL20 promote HCC progression

determined by quantitative Real-Time PCR (qRT-PCR) using SYBR Green reagent (TaKaRa) in a 7500 Fast Real-Time PCR system (Life Technology). The primer sequences were provided in [Supplementary Table 1](#). Immunohistochemistry (IHC) of rabbit anti-human CCL20 polyclonal antibodies (PeproTech, Cat. #500-P95A) was used to determine CCL20 expression in HCC tissues according to the manufacturer's instructions. Briefly, deparaffinized tissue sections were treated by 3% hydrogen peroxide after antigen retrieval in 0.01 M citrate buffer, at pH 6, for 15 min. The sections were blocked by using normal goat and rabbit serum mixture for 30 min and then incubated with anti-CCL20 polyclonal antibodies at 4°C overnight. After washing, the section were then stained with VECTASTAIN Elite ABC system (Vector Labs) and colored with 3-amino-9-ethylcarbazole.

Immunohistochemistry (IHC)

For CD19 staining in human HCC samples, the antigens were retrieved in 0.01 M Tris/EDTA buffer (pH 9.0) for 15 min, followed by treatment with the alkaline phosphatase (AP) inhibitor (Biodragon, Beijing, China) for 15 min. Specimens were incubated at 4°C with 1:50 diluted mouse anti-human CD19 monoclonal antibody (ZSGB-Bio, Beijing, China) overnight. The sections were then incubated with commercially optimized AP-labeled goat anti-mouse IgG antibody at room temperature for 30 min and colored with AP-Red solution for 12 min (all reagents from ZSGB-Bio, Beijing, China). For CD31 staining in human HCC samples and mouse lung tissues, specimens were incubated at 4°C with 1:100 diluted rabbit anti-human and mouse CD31 polyclonal antibody (Abcam) overnight. The sections were then incubated with horseradish peroxidase (HRP)-conjugated goat anti-rabbit antibody and colored with 3, 3'-diaminobenzidine (DAB) solution (all reagents from ZSGB-Bio, Beijing, China). These sections were scanned and analyzed by Aperio ScanScope and Console software version 12 (Aperio Technologies).

Determination of CCR6 by flow cytometry (FCM)

CCR6 transcriptional levels in HCC tissues were determined by qRT-PCR using SYBR Green reagent (TaKaRa) with the primers provided in

[Supplementary Table 1](#). To investigate the CCR6 expression on different cell population in the HCC tissues, 5×10^6 single cells from fresh sectioned HCC tissues were prepared as our previous report [17] and double stained with FITC-conjugated mouse anti-human CD45 and PE-conjugated mouse anti-human CCR6 antibodies (eBioscience). To detect the expression of CCR6 on different cell lines, PE-conjugated mouse anti-human CCR6 or PE-conjugated Armenian hamster anti-mouse CCR6 antibody (BioLegend) was added into 1×10^6 single cell suspension. To analyze the expression of CCR6 on different murine B cell subsets, 1×10^6 single splenocytes were prepared and triple stained with PE-conjugated rat anti-mouse CD19, FITC-conjugated rat anti-mouse CD5 and APC-conjugated Armenian hamster anti-mouse CCR6 antibodies (all from BioLegend). All the Data were acquired in LSR-II (BD Biosciences) and analyzed by using Flowjo software.

Chemotaxis assay on tumor cell-derived CCL20

Tumor conditioned medium (TCM) collected from murine hepatoma cell line H22 or normal culture medium was treated with 10 µg/ml rat anti-mouse CCL20 neutralizing antibodies (R&D systems) or rat IgG₁ at 37°C for 30 minutes. In lower chambers of transwells (5 µm pore size, Corning), 600 µl treated medium were added, and in upper chambers, 1×10^6 whole splenocytes or sorted CD19⁺ B cells in 100 µl culture medium were added. Each condition was triplicated. The cells with medium alone was used as spontaneous migration. After incubation at 37°C for 2 hours, the migrated cells in the lower chambers were collected, counted and double-stained with FITC-conjugated rat anti-mouse B220 (eBioscience) and PE-conjugated Armenian hamster anti-mouse CD3 antibodies (BioLegend) or with FITC-conjugated rat anti-mouse CD5 antibody when sorted CD19⁺ B cells were added. The stained cells were analyzed by using FCM.

Cell sorting and tube formation assay

Splenocytes from Balb/c mouse were stained with PE-conjugated rat anti-mouse CD19 and sorted for CD19⁺ cells by using FACS Aria III (BD Biosciences). 1×10^6 CD19⁺ B cells in 100 µl were plated in the upper chamber of a transwell (5 µm pore size) and 600 µl condition medium of H22 cells with 50 ng/ml mouse recombinated

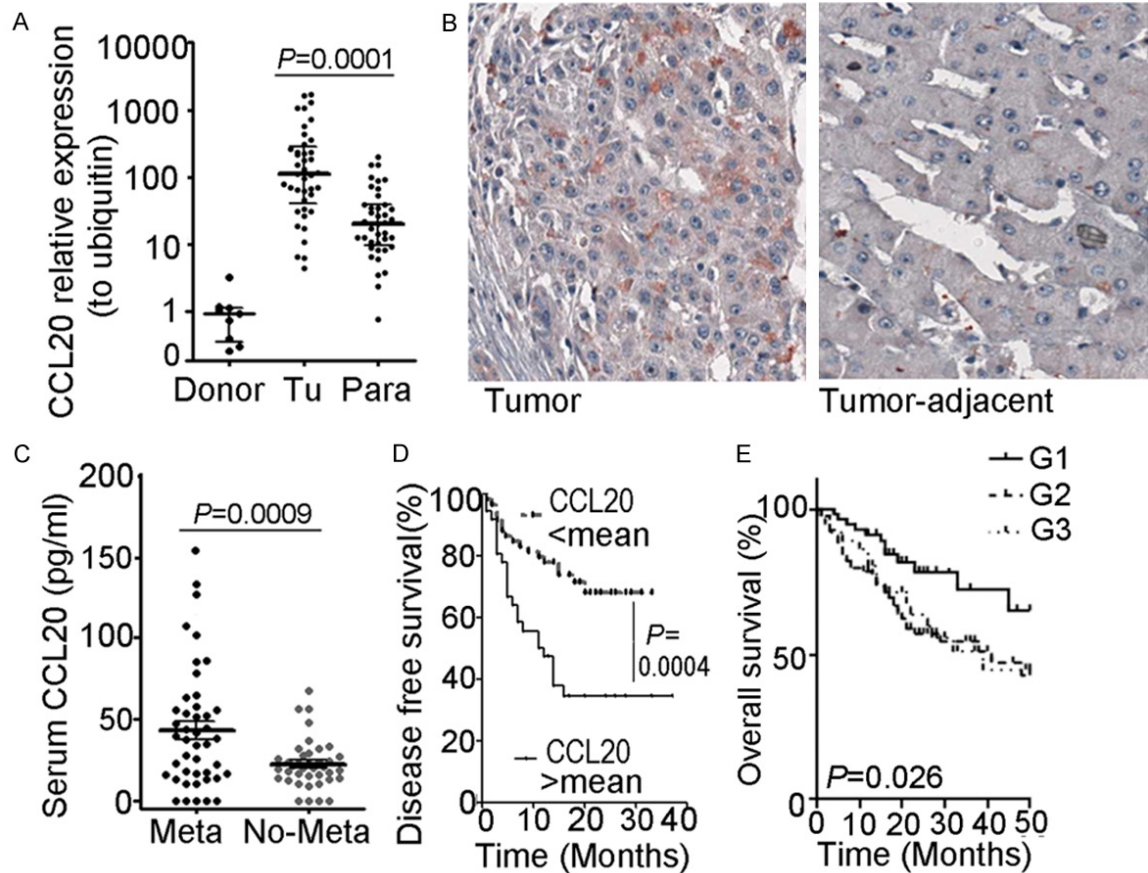


Figure 1. Expression of CCL20 in HCC patients and disease metastasis. A. CCL20 mRNA expression was measured by qRT-PCR in 41 pairs of HCC (Tu) and matched adjacent no-tumor (Para) tissues, and healthy hepatic (Donor) tissues from 6 liver donors. Ubiquitin mRNA served as an internal control. B. Representative CCL20 staining by using immunohistochemistry in HCC tumor tissues and adjacent no-tumor tissues. C. CCL20 concentration in the pre-therapy serum of 95 HCC cases from CH-CAMS were determined by ELISA. After being followed for 3 years, 50 cases had metastasis (Meta) and 45 cases did not have metastasis (No-Meta). D. Kaplan-Meier estimated patients' disease-free survival based on the mean value of serum CCL20 levels in the CH-CAMS cohort (95 cases). E. Kaplan-Meier estimated patients' overall survival based on the mean value of serum CCL20 levels and tumor size in two combined cohorts from CH-CAMS (95 cases) and from Henan Cancer Provincial Hospital (85 cases) with a median follow-up period of 19 months. G1: tumor size ≤ 5 cm in diameter and serum CCL20 \leq mean; G2: tumor size > 5 cm in diameter or serum CCL20 $>$ mean; G3: tumor size > 5 cm in diameter and serum CCL20 $>$ mean. The $P=0.026$ by log-rank test. Data were presented as mean \pm SD.

CCL20 protein (PeproTech) were added into the lower chamber. After incubation at 37°C for 2 hours, the cells from upper and lower chamber were collected, respectively. For tube formation assay, 3×10^4 HUVEC were mixed with the sorted CD19⁺ B cells, or with the lower chamber B cells or with the upper chamber B cells at 1:1 ratio, respectively. The cell mixtures in 100 μ l DMEM medium containing 5% FBS were then plated onto the neutralized collagen. After being cultured for 16 hours the cells were fixed with 4% paraformaldehyde for 10 min, washed, and analyzed under an inverted light microscope (Leica). Closed networks of vessel-like tubes were counted from each well [14, 15].

Monitor the tumor growth and metastasis in vivo

To determine the effect of secreted CCL20 on tumor growth, 1×10^6 Hepa1-6 cells in 100 μ l PBS solution with or without 150 ng recombinant murine CCL20 protein were injected subcutaneously into male C57BL/6 mice (6 weeks old). On the day 7, day 14, and day 21 after tumor cell injection, 20 μ l saline containing 150 ng recombinant CCL20 protein or 150 ng BSA was injected into the tumor bed of each mouse respectively.

To determine the tumor cell growth after blocking the CCL20, 5×10^4 H22 cells in 50 μ l PBS

CCR6⁺ B lymphocytes recruited by tumor-secreted CCL20 promote HCC progression

solution with 50 µg rat IgG₁ or rat anti-mouse CCL20 neutralizing antibodies were inoculated subcutaneously into male Balb/C mice or SCID mice, respectively. Tumor size was measured every 3-5 days. The tumor volume was calculated by length×width²×0.5 [18].

To determine the tumor growth after blocking the B cells infiltration, 5×10⁴ H22 cells in 50 µl PBS were injected into left lateral lobe of the liver of Balb/C mice. One and three days after tumor cell inoculation, each mouse received 50 µg rat IgG₁ or rat anti-CD20 neutralizing antibodies through intraperitoneal injection. Liver nodules were quantified on day 10.

To determine the tumor cell metastasis after blocking the CCL20, 1×10⁶ H22 cells in 0.2 ml PBS were intravenously inoculated into the Balb/C mice. On the day 1 and day 4 after the H22 tumor cell inoculation, each mouse received 100 µg rat IgG₁ or rat anti-CCL20 neutralizing antibodies through intraperitoneal injection. Lung metastasis nodules were quantified on day 21, and the lung tissues were fixed in formalin. The sectioned tissues were stained with haematoxylin and eosin. Microvesicular density in metastatic tumors was determined by staining of CD31.

Statistical analysis

All statistical analyses were performed using SPSS 18.0. Student *t* tests and ANOVA analysis were used to compare the paired data and data of multiple groups, respectively. Mann-Whitney *U* tests were conducted to compare the non-parametric data. Categorical data were compared by using χ^2 tests or Fisher's exact tests. Pearson's correlation tests were used to examine the associations between the expression levels of CCL20 and CCR6. Log-rank tests were used to determine significance of survival data in the Kaplan-Meier curve. A *P*-value of less than 0.05 was considered to be statistically significant.

Results

HCC tumor tissues over produce CCL20

CCL20 can be constitutively produced in low levels by various cell types including hepatocyte and inflammatory cells [19]. To confirm the over-production in the HCC cells, we analyzed the CCL20 mRNA transcription by using qRT-

PCR in 41 pairs of HCC and adjacent non-tumor tissues, that were derived from CH-CAMS cohort, and normal hepatic tissues from 6 healthy donors. Compared to the healthy livers, both the tumorous and adjacent non-tumor tissues showed higher expression of CCL20 (**Figure 1A**). Nevertheless, CCL20 expressing levels were significantly increased in tumorous tissues than in non-tumor tissues (**Figure 1A**). By using immunohistochemistry (IHC) staining we found that CCL20-positive cells were mainly recognized in the tumorous tissues (n=15) and some of the HCC cells were highly stained with anti-CCL20 antibodies. CCL20-positive cells were negligibly distributed within the no-tumor tissues (**Figure 1B**).

We then quantified the pretherapy serum CCL20 levels in 95 HCC patients who received curative hepatectomy in the CH-CAMS. Fifty patients had metastasis after being followed for 3 years. Their CCL20 serum levels showed significantly higher than those without the metastasis (**Figure 1C**). By using the mean concentration of the CCL20 in all the HCC patients, we found that the disease free survival rate in the cases with higher levels of serum CCL20 was significantly lower than in those with lower levels of serum CCL20 (**Figure 1D**).

To validate the effect of CCL20 on HCC progression we determined the serum CCL20 concentration in another HCC cohort from Henan Provincial Cancer Hospital and analyzed the overall survival in all the HCC patients. The patients with higher serum CCL20 concentration showed substantially worse overall survival than those with lower serum CCL20 concentration (**Figure 1E**). These data suggested that overproduction of CCL20 in HCC greatly affected the disease progression.

CCL20 expression in HCC is positively correlated with the infiltration of CCR6-positive cells

When we cultured the HCC cell lines (Hep3B, HepG2 and Huh7), and murine hepatoma cell lines (Hepa1-6, H22) in the presence or absence of recombinant CCL20 protein, we found no significant differences in cell migration and proliferation (data not shown). We also observed no differences in the cell proliferation and migration after the neutralizing antibodies against CCL20 were added in the cell culture medium (**Supplementary Figure 1**). These data

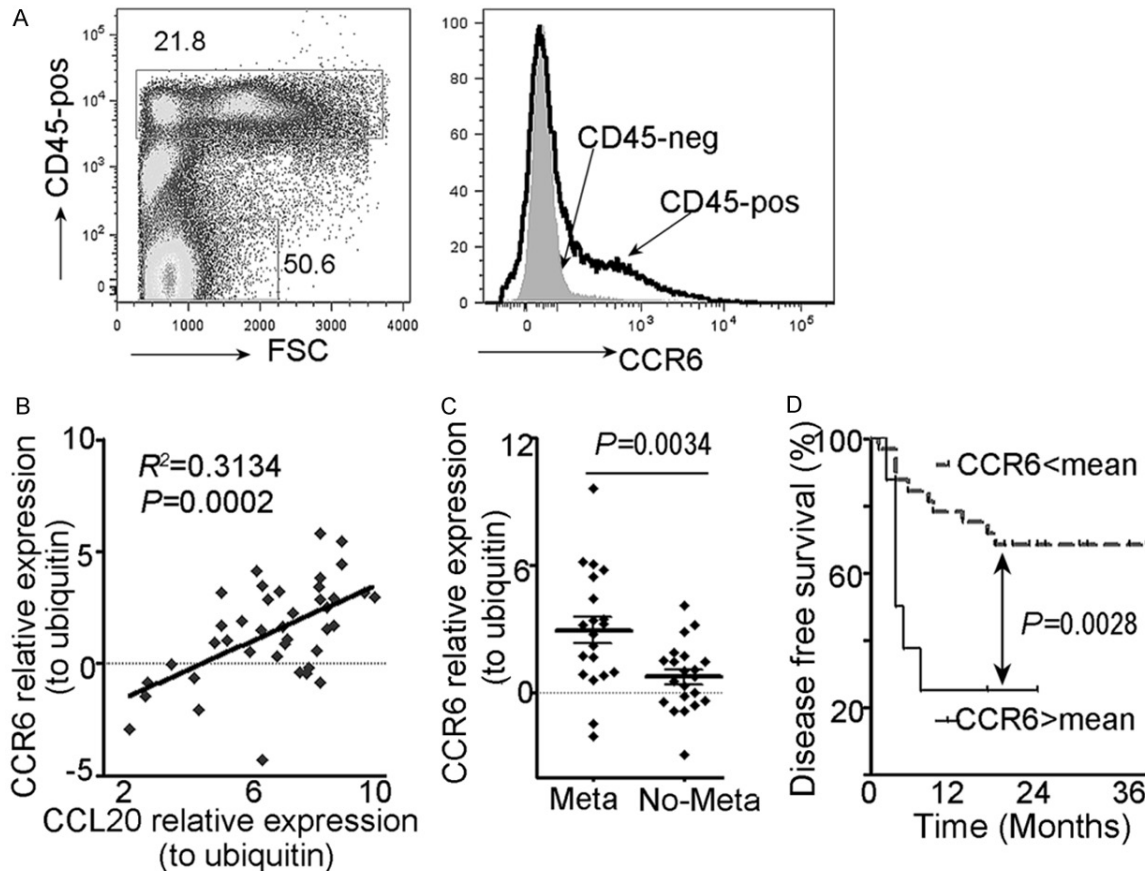


Figure 2. Expressions of CCR6 in HCC tissues and disease metastasis. A. Expression of CCR6 in HCC tissues analyzed by FCM after the single cells were prepared. Representatives of six independent patients. B. Pearson's analysis of correlation between CCL20 and CCR6 mRNA expression levels determined by qRT-PCR in 41 HCC cases. C. CCR6 mRNA expression levels were determined by qRT-PCR in 41 HCC cases with (n=20) or without (n=21) metastasis. Ubiquitin mRNA served as an internal control. Meta: metastasis; No-Meta: non-metastasis. D. Kaplan-Meier estimates patients' disease-free survival (DFS) based on the mean value of CCR6 levels, with a median follow-up period of 20 months. Data were presented as mean \pm SD.

indicated that the direct effect of CCL20 on tumor cell might be subtle.

CCR6 is the exclusive high affinity receptor for CCL20, we then examined the expression of CCR6 in HCC cell lines, murine hepatoma cell lines and the human HCC tissues. All the tumor cells showed negligible expression of CCR6 (Figure 2A and Supplementary Figure 2). Instead, CCR6 were mainly detected on the CD45-positive intrahepatic immune cells of HCC tissues (Figure 2A). We therefore hypothesized that the tumor cell-derived CCL20 supported HCC progression through recruiting different types of immune cells. To validate the effect of tumor cell-derived CCL20 in recruiting CCR6-expressing immune cells that in turn supported the HCC progression, we evaluated the

correlation between CCL20 and CCR6 in the aforementioned 41 HCC tissues. Pearson's analysis showed that CCL20 expression was positively correlated with the CCR6 in HCC tumor tissues ($R^2=0.3134$, $P=0.0002$) (Figure 2B). To generalize the association of CCR6 and CCL20 in HCC, we further examined the correlation of CCL20 and CCR6 gene expression data in large cohorts of HCC patients, which are available from the public database (GSE9843, GSE14520, GSE16757 and GSE25097). In all the data sets, CCR6 expression was found significantly correlated with that of CCL20 (Supplementary Figure 3).

Further analysis conducted in the aforementioned 41 tumor tissues indicated that the HCC patients with distal metastasis had higher lev-

CCR6⁺ B lymphocytes recruited by tumor-secreted CCL20 promote HCC progression

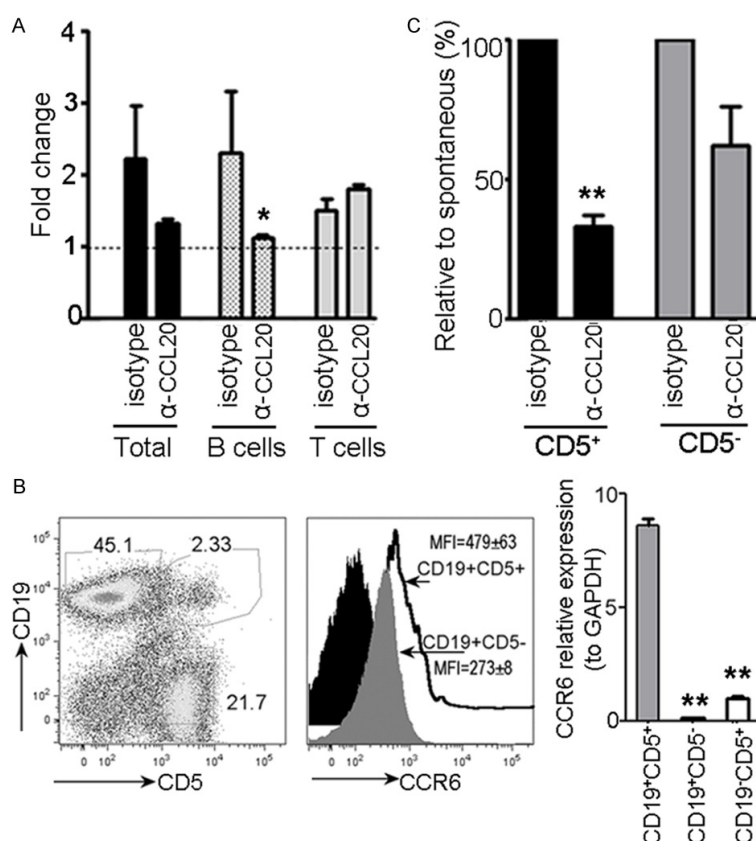


Figure 3. Tumor cell derived-CCL20 recruits CD19⁺CD5⁺ B cells via CCR6. (A) Tumor conditioned medium from murine hepatoma cell line H22 was collected and treated with 10 μg/ml rat anti-mouse CCL20 (α-CCL20) or the same amount of rat IgG₁ (isotype) for 30 minutes. The chemotaxis assay on murine splenocytes was then conducted for 2 hours by using a transwell with 5-μm pore size. The numbers of migrated cells in the lower chambers were collected, counted and stained with FITC-conjugated B220 and PE-conjugated CD3 for FCM analysis. Normal culture medium with cells only was used as spontaneous migration. Data were presented as the fold changes related to the spontaneous migration. Experiments were repeated twice. (B) The splenocytes were stained with PE-conjugated CD19, FITC-conjugated CD5 and APC-conjugated CCR6 and analyzed by FCM (left panel). Data were the representatives of 3 independent experiments. The splenocytes stained with PE-conjugated CD19 and FITC-conjugated CD5 were sorted into 3 population: CD19⁺CD5⁺, CD19⁺CD5⁻, and CD19⁻CD5⁺ by FACS Aria II. The CCR6 mRNA expression was quantified by qRT-PCR (right panel). (C) The CD19⁺ B cells were sorted from splenocytes and chemotaxis assay was conducted as described in (A). The numbers of migrated cells in the lower chambers were collected and counted and stained with FITC-conjugated CD5 for FACS analysis. Data were presented as mean ± SD. *, P<0.05; **, P<0.001.

els of CCR6 expression than those without metastasis (**Figure 2C**). Using the mean expressing levels of CCR6 from all the HCC patients we found that the patients with increased infiltration of CCR6-expressed cells in HCC tissues showed a poorer prognosis (**Figure 2D**). These results indicated that increased infiltration of CCR6⁺ immune cells in

response to tumor cell-derived CCL20 supported the HCC progression.

Blocking tumor cell derived-CCL20 inhibits the recruitment of CD19⁺CD5⁺ B lymphocytes

It was found that CCR6⁺ B cells could enter inflamed tissues in which CCL20 expressed [20]. To investigate the role of CCR6⁺ B cells in response to the tumor cell-derived CCL20, we conducted a chemotaxis assay on murine splenocytes. The murine hepatoma H22 cell line was found to constitutively produce certain amount of CCL20 (**Supplementary Figure 4**). When tumor conditioned medium was treated with anti-CCL20 neutralizing antibodies, the migration of B lymphocytes was significantly inhibited. However, the percentage of recruited CD3-positive cells increased to some extent (**Figure 3A**).

Several studies have documented the important roles of B lymphocytes in promoting cancer progression [13, 14]. Recently, it was found that CD19⁺CD5⁺ B cells increased significantly in tumors and this subset of B cells promoted the tumor growth [14]. We then determined the CCR6 expression on this subset of B cells. FACS analysis of mouse splenocytes showed that the

CCR6 expression level in CD19⁺CD5⁺ cells was significantly higher than that of CD19⁺CD5⁻ B cells (**Figure 3B**). We also sorted the CD19⁺CD5⁺, CD19⁺CD5⁻, and CD19⁻CD5⁺ cells and quantified their CCR6 mRNA levels. qRT-PCR analysis showed that the CD19⁺CD5⁺ B cells had higher CCR6 mRNA levels than other two cell population (**Figure 3B**).

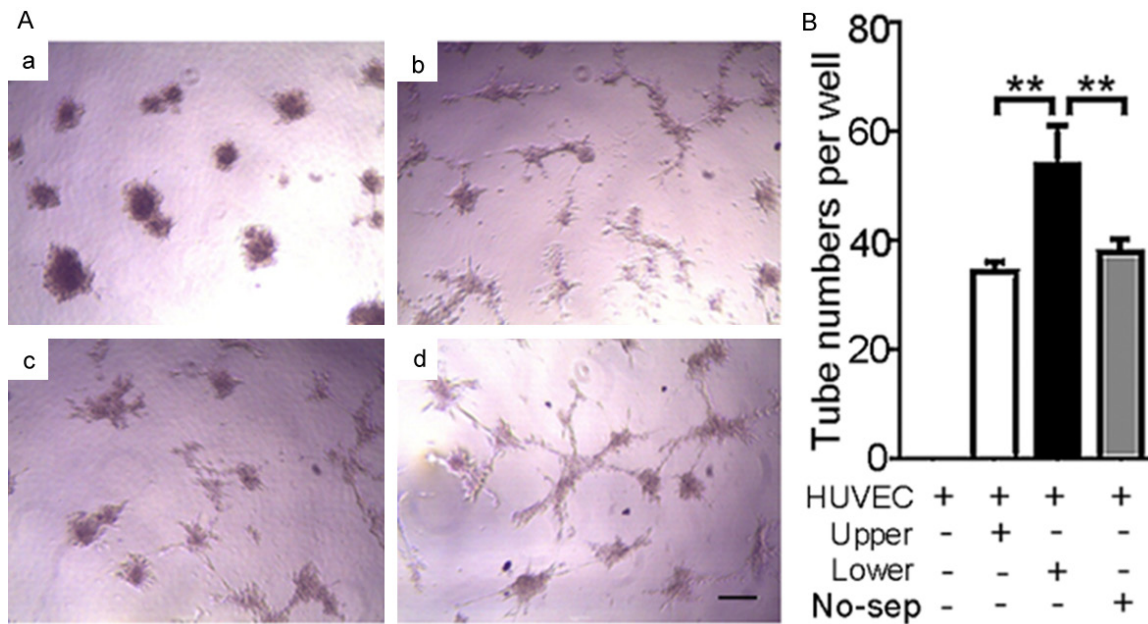


Figure 4. CCL20 reposing B cells promote endothelial cell tube formation. (A) Representative images of tube formation by co-culturing the HUVECs with different CD19⁺ B cells. (a) HUVECs only; (b-d) HUVECs were co-cultured with un-separated CD19⁺ B cells (b) or with B cells collected from un-migrated upper chambers (c) or with B cells collected from migrated lower chambers (d) at 1:1 ratio. Bar, 2 μ m. (B) The average number of vessel-like structures formed by HUVECs after co-culture with the indicated B cells (n=5). Upper: un-migrated upper chamber B cells; Lower: migrated lower chamber B cells; No-sep: total CD19⁺ B cells. Data were presented as mean \pm SD, **, $P < 0.001$.

We further sorted the CD19⁺ B cells and conducted the chemotaxis assay using the tumor conditioned medium collected from H22 cells. When CCL20 activity was blocked by anti-CCL20 neutralizing antibodies, the migration of CD19⁺CD5⁺ B cells was more dramatically inhibited than that of the CD19⁺CD5⁻ B cells (**Figure 3C**). These data indicated that CD19⁺CD5⁺ B cell subset was an important responder to the tumor cell-derived CCL20 to support the HCC development.

CCL20 responding B cells support the angiogenesis

HCC is typically a hypervascular tumor, and microvascular invasion is the most important risk factor for HCC distal metastasis [21]. We then analyzed the angiogenesis capacity of B cells that were recruited to the tumor conditioned medium containing CCL20. The sorted CD19⁺ B cells were added into the upper chamber of a transwell in the tumor conditioned medium for 2 hours, and the migrated B cells in the low chamber or un-migrated B cells in the upper chambers were then co-cultured with HUVEC cells for 16 hours. The tube numbers of the HUVEC co-cultured with the migrated B

cells was significantly higher than that of HUVEC with the un-migrated upper chamber B or with total CD19⁺ B cells (**Figure 4**). This result indicated that the CCL20 responding B cells had higher capacities to support the angiogenesis.

Neutralizing CCL20 activities in immunocompetent but not in SCID mice inhibits tumor growth and metastasis

We then analyzed the effect of CCL20 on tumor growth and metastasis *in vivo*. After the H22 cells were inoculated into Balb/C mice via subcutaneous injection, each mouse received 50 μ g rat anti-mouse CCL20 neutralizing antibodies (n=8), or the same amount of rat IgG₁ (n=12) twice in the first week. Twenty days after the tumor cell injection, all the mice without any treatment (n=5, data not shown) and 11/12 (91.7%) mice that received the rat IgG₁ developed tumors. However, only 4 of 8 mice (50%) that received anti-mouse CCL20 neutralizing antibodies developed tumors. Tumor growth in the anti-CCL20 antibody treated mice was slower compared with those received the rat IgG₁ (**Figure 5A**). In the SCID mice, which have no T cells and B cells, the tumor incidence rate and tumor volume had marginal difference

CCR6⁺ B lymphocytes recruited by tumor-secreted CCL20 promote HCC progression

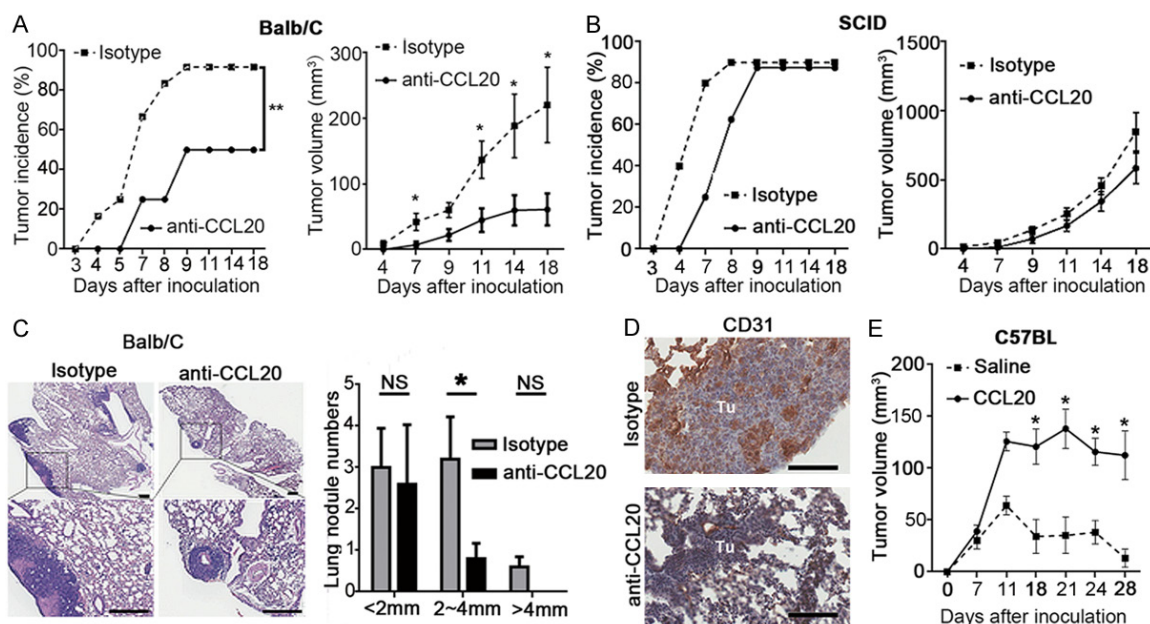


Figure 5. Blockade of CCL20 attenuates the tumor growth and metastasis in immunocompetent mice. **A.** 5×10^4 H22 cells in 50 μ l PBS were subcutaneously injected into Balb/C mice and treated with 50 μ g anti-CCL20 neutralizing antibodies or rat IgG₁ (as isotype control) twice in the first week after inoculation. Tumor incidence rate (left panel) and tumor volume (right panel) were shown for the group of mice ($n=12$ for rat IgG₁ group and $n=8$ for anti-CCL20 group). **B.** 5×10^4 H22 cells in 50 μ l PBS were subcutaneously implanted into SCID mice and treated with 50 μ g anti-CCL20 neutralizing antibodies or rat IgG₁ twice in the first week after inoculation. Tumor incidence rate (left panel) and tumor volume (right panel) were shown for the group of mice ($n=10$ for rat IgG₁ and $n=8$ for anti-CCL20 group). **C.** Representatives images of the lung histology of Balb/C mice that received 1×10^6 H22 cells in 0.2 ml PBS through intravenous injection and treated with 100 μ g anti-CCL20 neutralizing antibodies or rat IgG₁ (as isotype control) twice in the first week. Scale bars, 400 μ m (left panel). The numbers of metastatic nodules in the lungs were shown for the group of mice (right panel, $n=5$ for each group). NS: No significant difference. **D.** Representative of CD31 immunohistochemistry staining in lung tissues of the mice that were treated with rat IgG₁ or with anti-CCL20 neutralizing antibodies. Tu: tumor nodule. Scale bars, 100 μ m. **E.** 1×10^6 Hepa1-6 cells in 100 μ l PBS were subcutaneously injected into C57BL/6 mice, then the mice were treated with 150 ng BSA in 20 μ l saline or with 150 ng recombinant murine CCL20 protein in 20 μ l saline every week. The tumors at indicated time points were measured for each mice ($n=5$ for saline group and $n=6$ for CCL20 group). Data were presented as mean \pm SEM. *, $P < 0.05$.

between IgG₁ treated group ($n=10$) and anti-CCL20 antibody treated group ($n=8$) (**Figure 5B**).

We also investigated the tumor metastasis after blocking the CCL20 activities. After H22 cells were injected into Balb/C mice intravenously (D0), each mouse received 100 μ g rat anti-mouse CCL20 neutralizing antibodies on D1 and D4 ($n=5$) or the rat IgG₁ ($n=5$) at the same time points. On D28, all the mice received rat IgG₁ or the mice without any treatment ($n=5$, data not shown) developed lung metastasis. However, only 3 mice (60%) which received the anti-CCL20 neutralizing antibodies displayed the surface lesions in the lungs. Quantification of the surface lesions in the lungs showed the tumor numbers and tumor size in the mice that received anti-CCL20 neutralizing antibodies

dramatically decreased compared with the mice that received the rat IgG₁ (**Figure 5C**). We observed no effect of the anti-CCL20 neutralizing antibodies in decreasing the tumor metastasis in the SCID mice (**Supplementary Figure 5**).

As the capacity of the CCL20 responding B cells in supporting angiogenesis, we then analyzed the microvascular density in lung metastatic tissues from the mice that received rat IgG₁ or anti-CCL20 neutralizing antibodies. The CD31 staining in the lung tissues from anti-CCL20 antibody treated group decreased apparently compared with the rat IgG₁ treated group (**Figure 5D**). To eliminate the effect of subtle amount of CCL20 produced by some other cells on tumor growth, we used another murine hepatoma cell line, Hepa1-6 cells that had unde-

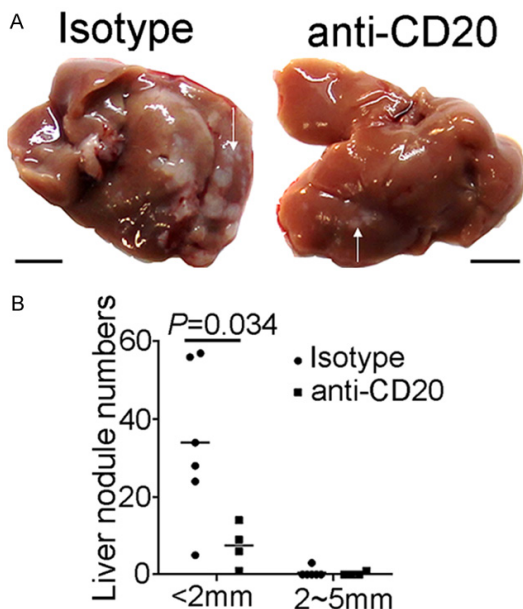


Figure 6. Depletion of B lymphocytes attenuates the tumor growth in immunocompetent mice. A. Representative image of gross liver of Balb/C mice. A total of 5×10^4 H22 cells in 50 μ l PBS were injected into left lateral lobe of the livers of Balb/C mice. Each mouse received 50 μ g rat anti-mouse CD20 (n=4) via intraperitoneal injection on D1 and D4, respectively. Same amount of rat IgG₁ (n=6) were injected at the same time points as a control. All the mice were sacrificed at D10 and the liver tumor nodules were quantified. Scale bars, 0.5 mm. B. The numbers of tumor nodules in the liver were shown for the groups of mice (n=6 for control group and n=4 for anti-CD20 neutralizing antibodies treated group).

tectable CCL20 secretion (Supplementary Figure 4), to confirm our findings. After the Hepa1-6 cells being injected subcutaneously into syngeneic C57BL/6 mice, 150 ng recombinant CCL20 protein (n=6) or 150 ng BSA in 20 μ l saline (n=5) was injected into the tumor bed once a week for three weeks. In the mice that received the BSA/saline, detectable tumor mass formed in 5-7 days after Hepa1-6 cell injection and peaked in 10-12 days. The formed tumors decreased gradually in size after day 12-14 and vanished within 28 days. This tumor growth trend was also observed in the mice without any treatment (data not shown). However, in the mice that received the same amount of CCL20/saline, the tumor growth was stable in the mice (Figure 5E).

Depletion of B lymphocyte infiltrating in immunocompetent mice attenuates tumor growth

Several types of immune cells have been documented to express CCR6, including T cells, B

cells, macrophages and NK cells [10, 12]. To confirm the effect of B cells in promoting liver cancer, we injected H22 hepatoma cells into left lateral lobe of the livers of Balb/C mice to mimic the tumor milieu of HCC development. When the B cells were depleted by using anti-CD20 neutralizing antibodies (n=4), tumor growth was significantly inhibited compared with that in the mice that received the rat IgG₁ (n=6) isotype (Figure 6). This data suggested blocking the B cells that response to tumor secreted CCL20 could attenuate HCC growth *in vivo*.

To further confirm the effect of infiltrated B cells in supporting angiogenesis for HCC progression, in human HCC tissues (n=13), we stained the markers of B cells (CD19) and blood vessels (CD31). Analysis under microscopy showed that CD19⁺ B cells tended to accumulate around microvessels instead of distributing evenly throughout the tumor tissues (Supplementary Figure 6).

Discussion

Chemokines generated by infiltrating leukocytes, resident stromal cells or tumor cells are important mediators in tumor progression. These soluble molecules are able to guide the infiltration of different types of leukocytes that shape the tumor growth [11, 22]. In this study, we found that CCL20 was significantly up-regulated in most of HCC tissues and elevation of pretherapy serum CCL20 was closely associated with tumor metastasis and patient survival times. HCC cell-derived CCL20 was able to recruit CCR6-expressing CD19⁺CD5⁺ B lymphocytes, which in turn supported the tumor progression through enhancing angiogenesis. HCC growth and metastasis were inhibited significantly after blocking CCL20 activity in the immunocompetent mice but not in the immunodeficient mice. Malignant transformed hepatocytes were an important source of elevated serum CCL20 in HCC patients and elevation of pretherapy serum CCL20 might be a potential marker for HCC progression prediction and a potential target for HCC relapse intervention.

Several studies documented that both tumor cells and tumor-associated macrophages were able to produce CCL20 *in vivo* [12, 23-25]. Our previously study found that the up-regulation of CCL20 was associated with the mutation of TP53 and the over-expression of CCL20 was

one of the “stemness” trait in HCC [8]. In the present study, we found that CCL20 was significantly up-regulated in most HCC tissues and some of the HCC cells were highly stained of CCL20. It is unclear how the CCL20 affects the disease progression. In cell culture system we found slight effects of CCL20 directly on cell proliferation and metastasis. Expression of CCR6, the sole selective chemokine receptor for CCL20, was detected negligibly on the HCC tumor cells. We therefore hypothesized that the HCC cell-derived CCL20 affected the HCC progression through recruiting CCR6-expressing leukocytes which in turn affected the disease progression. Indeed, the CD45-positive intra-hepatic immune cells of HCC tissues were found to be the dominant CCR6-expressing cells. Moreover, both our results and public gene expression profiling data of large HCC patient cohorts (GSE9843, GSE14520, GSE-16757 and GSE25097) demonstrated positive correlation between the expression of CCR6 and CCL20. The HCC tissues with metastatic potential and adverse outcome showed higher CCR6-expressing levels than the non-metastatic cases. Notably, a study from Liang’s group reported that monocyte-derived macrophages in response to the HCC cell-derived CCL20 suppressed the proliferation of effector T cells and promoted the expansion of immunosuppressive regulatory T cells to accelerate the tumor metastasis via HIF-1 α /CCL20/IDO axis [10].

In addition to the macrophages, CCR6 has been confirmed to be expressed on the effector/memory T cells, B cells, and NK cells [12]. The presence of “ectopic lymphoid-like structures (ELS)”, which contained heterogeneous immune cells, has been widely observed in different cancers [26]. The poor prognosis of HCC was found closely associated with higher density of ELS, which facilitated the malignant hepatocyte progenitor cells by providing a cellular and cytokine milieu for tumor survival and proliferation [27]. Our results presented here demonstrated that the recruitment of B cells by tumor conditioned medium was dramatically inhibited by anti-CCL20 neutralizing antibodies, indicating that the B leukocytes were important responders to the HCC tumor cell-derived CCL20. Oncogenic potential of B cell malignancies had been reported to be promoted by CD5 and STAT3 feed-forward loop [14]. This was consistent with our results which showed that

the expression of CCR6 were apparently up-regulated in CD19⁺CD5⁺ B cell subset compared with the CD19⁺CD5⁻ B cells or CD19⁻ cells. When the CCL20 activity was blocked, the recruitment of CD19⁺CD5⁺ B cells was mainly inhibited, while it showed moderate effect on CD19⁺CD5⁻ B cells, indicating that the CD19⁺CD5⁺ B cell subset was an important responder to the tumor cell-derived CCL20.

Tumor associated B cells were found to contribute to tumor development through promoting tumor angiogenesis [15]. Our angiogenesis assays showed that CCL20 responding B cells effectively facilitated the angiogenesis compared with the CCL20 non-responding B cells. After blocking the CCL20 activities *in vivo* tumor metastasis was inhibited, meanwhile the angiogenesis in tumor metastatic lung tissues was also reduced. Our current study by using the wild type immuno-component mice and the SCID mice, which have intact myeloid lineage (microphage, dendritic cells and granulocytes) but deficient in T and B cells, showed that the CCL20 activity was mainly affected in the immuno-component but not in the SCID mice. Moreover, depletion of B cells also suppressed the orthotopic growth of CCL20 expressed hepatoma. These results indicated the potential effect by manipulating all the immune cells in the tumor microenvironment to shaped the tumor growth in patients.

We observed that tumor-adjacent tissues had also increased CCL20 expression compared to the normal hepatic tissues. The reasons might be due to the infiltrated inflammatory cells, and the intrinsic changes in the tumor-adjacent hepatocytes. Several studies reported that variety of transcriptional factors including NF- κ B could bind to the CCL20 promoter region and mediate its transcription [28]. Therefore, the intrinsic genetic lesion that induced the hepatocyte malignant transformation, such as the TP53 mutation, NF- κ B activation, led to the upregulation of CCL20. The stem-cell-like cancer cells presented in the tumor-adjacent tissues which up-regulated expression of CCL20 might also be the potential seeds for tumor growth and metastasis.

In summary, the results from our current study indicated that HCC-derived CCL20 were able to recruit the CCR6-expressing CD5⁺ B cells, which in turn affected the disease progression.

Blockade of the interaction of CCL20 with CCR6 warranted further investigation as a potential therapeutic target and HCC relapse intervention.

Acknowledgements

The authors thank Dr. Huiguo Ding (Beijing YouAn Hospital) for providing normal hepatic tissues. This work was supported by National Basic Research Program of China (2013CB-910303), National Natural Science Foundation of China (30873397, 81672454) and CAMS Initiative for Innovative Medicine (2016-I2M-1-007).

Disclosure of conflict of interest

None.

Address correspondence to: Chunfeng Qu, State Key Laboratory of Molecular Oncology, National Cancer Center/Cancer Hospital, Chinese Academy of Medical Sciences & Peking Union Medical College, Beijing 100021, P. R. China. Tel: 8610-87783103; E-mail: qucf@cicams.ac.cn

References

[1] Poon D, Anderson BO, Chen LT, Tanaka K, Lau WY, Van Cutsem E, Singh H, Chow WC, Ooi LL, Chow P, Khin MW, Koo WH; Asian Oncology Summit. Management of hepatocellular carcinoma in Asia: consensus statement from the Asian Oncology Summit 2009. *Lancet Oncol* 2009; 10: 1111-8.

[2] Omata M, Lesmana LA, Tateishi R, Chen PJ, Lin SM, Yoshida H, Kudo M, Lee JM, Choi BI, Poon RT, Shiina S, Cheng AL, Jia JD, Obi S, Han KH, Jafri W, Chow P, Lim SG, Chawla YK, Budihusodo U, Gani RA, Lesmana CR, Putranto TA, Liaw YF, Sarin SK. Asian Pacific Association for the Study of the Liver consensus recommendations on hepatocellular carcinoma. *Hepatology* 2010; 4: 439-74.

[3] Budhu A, Roessler S, Zhao X, Yu Z, Forgues M, Ji J, Karoly E, Qin LX, Ye QH, Jia HL, Fan J, Sun HC, Tang ZY, Wang XW. Integrated metabolite and gene expression profiles identify lipid biomarkers associated with progression of hepatocellular carcinoma and patient outcomes. *Gastroenterology* 2013; 144: 1066-75, e1.

[4] Hoshida Y, Villanueva A, Kobayashi M, Peix J, Chiang DY, Camargo A, Gupta S, Moore J, Wrobel MJ, Lerner J, Reich M, Chan JA, Glickman JN, Ikeda K, Hashimoto M, Watanabe G, Daidone MG, Roayaie S, Schwartz M, Thung S, Salvesen HB, Gabriel S, Mazzaferro V, Bruix J,

Friedman SL, Kumada H, Llovet JM, Golub TR. Gene expression in fixed tissues and outcome in hepatocellular carcinoma. *N Engl J Med* 2008; 359: 1995-2004.

[5] Chew V, Chen J, Lee D, Loh E, Lee J, Lim KH, Weber A, Slankamenac K, Poon RT, Yang H, Ooi LL, Toh HC, Heikenwalder M, Ng IO, Nardin A, Abastado JP. Chemokine-driven lymphocyte infiltration: an early intratumoural event determining long-term survival in resectable hepatocellular carcinoma. *Gut* 2012; 61: 427-38.

[6] Hernandez-Gea V, Toffanin S, Friedman SL, Llovet JM. Role of the microenvironment in the pathogenesis and treatment of hepatocellular carcinoma. *Gastroenterology* 2013; 144: 512-27.

[7] Charo IF, Ransohoff RM. The many roles of chemokines and chemokine receptors in inflammation. *N Engl J Med* 2006; 354: 610-21.

[8] Woo HG, Wang XW, Budhu A, Kim YH, Kwon SM, Tang ZY, Sun Z, Harris CC, Thorgeirsson SS. Association of TP53 mutations with stem cell-like gene expression and survival of patients with hepatocellular carcinoma. *Gastroenterology* 2011; 140: 1063-70.

[9] Hou KZ, Fu ZQ, Gong H. Chemokine ligand 20 enhances progression of hepatocellular carcinoma via epithelial-mesenchymal transition. *World J Gastroenterol* 2015; 21: 475-83.

[10] Ye LY, Chen W, Bai XL, Xu XY, Zhang Q, Xia XF, Sun X, Li GG, Hu QD, Fu QH, Liang TB. Hypoxia-induced epithelial-to-mesenchymal transition in hepatocellular carcinoma induces an immunosuppressive tumor microenvironment to promote metastasis. *Cancer Res* 2016; 76: 818-30.

[11] Schreiber RD, Old LJ, Smyth MJ. Cancer immunoeediting: integrating immunity's roles in cancer suppression and promotion. *Science* 2011; 331: 1565-70.

[12] Comerford I, Bunting M, Fenix K, Haylock-Jacobs S, Litchfield W, Harata-Lee Y, Turvey M, Brazzatti J, Gregor C, Nguyen P, Kara E, McColl SR. An immune paradox: how can the same chemokine axis regulate both immune tolerance and activation?: CCR6/CCL20: a chemokine axis balancing immunological tolerance and inflammation in autoimmune disease. *Bioessays* 2010; 32: 1067-76.

[13] Xiao X, Lao XM, Chen MM, Liu RX, Wei Y, Ouyang FZ, Chen DP, Zhao XY, Zhao Q, Li XF, Liu CL, Zheng L, Kuang DM. PD-1 High identifies a novel regulatory b cell population in human hepatoma that promotes disease progression. *Cancer Discov* 2016; 6: 546-59.

[14] Zhang C, Xin H, Zhang W, Yazaki PJ, Zhang Z, Le K, Li W, Lee H, Kwak L, Forman S, Jove R, Yu H. CD5 binds to interleukin-6 and induces a feed-forward loop with the transcription factor

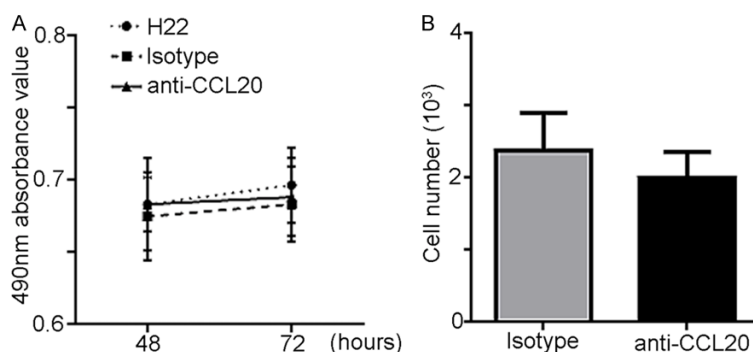
CCR6⁺ B lymphocytes recruited by tumor-secreted CCL20 promote HCC progression

- STAT3 in B cells to promote cancer. *Immunity* 2016; 44: 913-23.
- [15] Yang C, Lee H, Pal S, Jove V, Deng J, Zhang W, Hoon DS, Wakabayashi M, Forman S, Yu H. B cells promote tumor progression via STAT3 regulated-angiogenesis. *PLoS One* 2013; 8: e64159.
- [16] Duan Z, Gao J, Zhang L, Liang H, Huang X, Xu Q, Zhang Y, Shen T, Lu F. Phenotype and function of CXCR5+CD45RA-CD4+ T cells were altered in HBV-related hepatocellular carcinoma and elevated serum CXCL13 predicted better prognosis. *Oncotarget* 2015; 6: 44239-53.
- [17] Wu J, Du J, Liu L, Li Q, Rong W, Wang L, Wang Y, Zang M, Wu Z, Zhang Y, Qu C. Elevated pre-therapy serum IL17 in primary hepatocellular carcinoma patients correlate to increased risk of early recurrence after curative hepatectomy. *PLoS One* 2012; 7: e50035.
- [18] Euhus DM, Hudd C, LaRegina MC, Johnson FE. Tumor measurement in the nude mouse. *J Surg Oncol* 1986; 31: 229-34.
- [19] Schutyser E, Struyf S, Van Damme J. The CC chemokine CCL20 and its receptor CCR6. *Cytokine Growth Factor Rev* 2003; 14: 409-26.
- [20] Paradis M, Mindt BC, Duerr CU, Rojas OL, Ng D, Boulianne B, McCarthy DD, Yu MD, Summers deLuca LE, Ward LA, Waldron JB, Philpott DJ, Gommerman JL, Fritz JH. A TNF-alpha-CCL20-CCR6 axis regulates Nod1-induced B cell responses. *J Immunol* 2014; 192: 2787-99.
- [21] Zhu AX, Duda DG, Sahani DV, Jain RK. HCC and angiogenesis: possible targets and future directions. *Nat Rev Clin Oncol* 2011; 8: 292-301.
- [22] Grivennikov SI, Greten FR, Karin M. Immunity, inflammation, and cancer. *Cell* 2010; 140: 883-99.
- [23] Cheng XS, Li YF, Tan J, Sun B, Xiao YC, Fang XB, Zhang XF, Li Q, Dong JH, Li M, Qian HH, Yin ZF, Yang ZB. CCL20 and CXCL8 synergize to promote progression and poor survival outcome in patients with colorectal cancer by collaborative induction of the epithelial-mesenchymal transition. *Cancer Lett* 2014; 348: 77-87.
- [24] Du D, Liu Y, Qian H, Zhang B, Tang X, Zhang T, Liu W. The effects of the CCR6/CCL20 biological axis on the invasion and metastasis of hepatocellular carcinoma. *Int J Mol Sci* 2014; 15: 6441-52.
- [25] Wang GZ, Cheng X, Li XC, Liu YQ, Wang XQ, Shi X, Wang ZY, Guo YQ, Wen ZS, Huang YC, Zhou GB. Tobacco smoke induces production of chemokine CCL20 to promote lung cancer. *Cancer Lett* 2015; 363: 60-70.
- [26] Pitzalis C, Jones GW, Bombardieri M, Jones SA. Ectopic lymphoid-like structures in infection, cancer and autoimmunity. *Nat Rev Immunol* 2014; 14: 447-62.
- [27] Finkin S, Yuan D, Stein I, Taniguchi K, Weber A, Unger K, Browning JL, Goossens N, Nakagawa S, Gunasekaran G, Schwartz ME, Kobayashi M, Kumada H, Berger M, Pappo O, Rajewsky K, Hoshida Y, Karin M, Heikenwalder M, Ben-Neriah Y, Pikarsky E. Ectopic lymphoid structures function as microniches for tumor progenitor cells in hepatocellular carcinoma. *Nat Immunol* 2015; 16: 1235-44.
- [28] Zhao L, Xia J, Wang X, Xu F. Transcriptional regulation of CCL20 expression. *Microbes Infect* 2014; 16: 864-70.

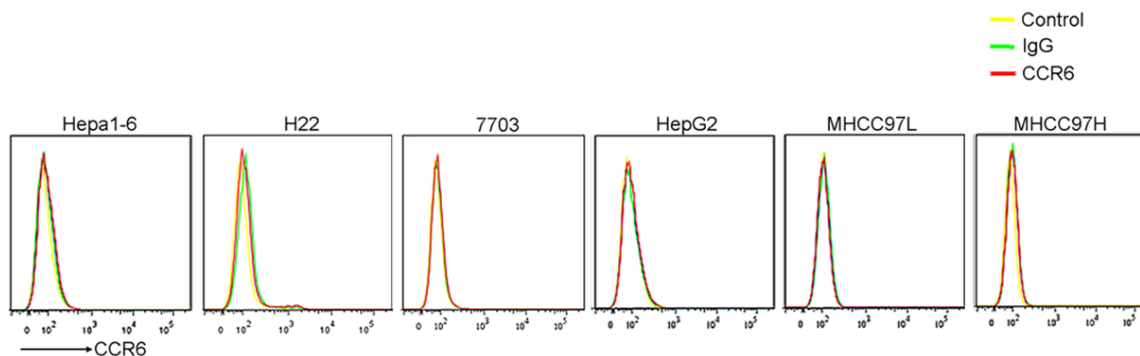
CCR6⁺ B lymphocytes recruited by tumor-secreted CCL20 promote HCC progression

Supplementary Table 1. RT-PCR primers

RT-PCR primers	Sequences
Ubiquitin F	ACTCGTTGCATAAATTTGCGCTC
Ubiquitin R	CGAAGATCTGCATTTTGACCTGTT
CCL20 F	TGCTGTACCAAGAGTTTGCTC
CCL20 R	CGCACACAGACAACCTTTTCTTT
CCR6 F	CCATTCTGGGCAGTGAGTCA
CCR6 R	AGCAGCATCCCGCAGTTAA

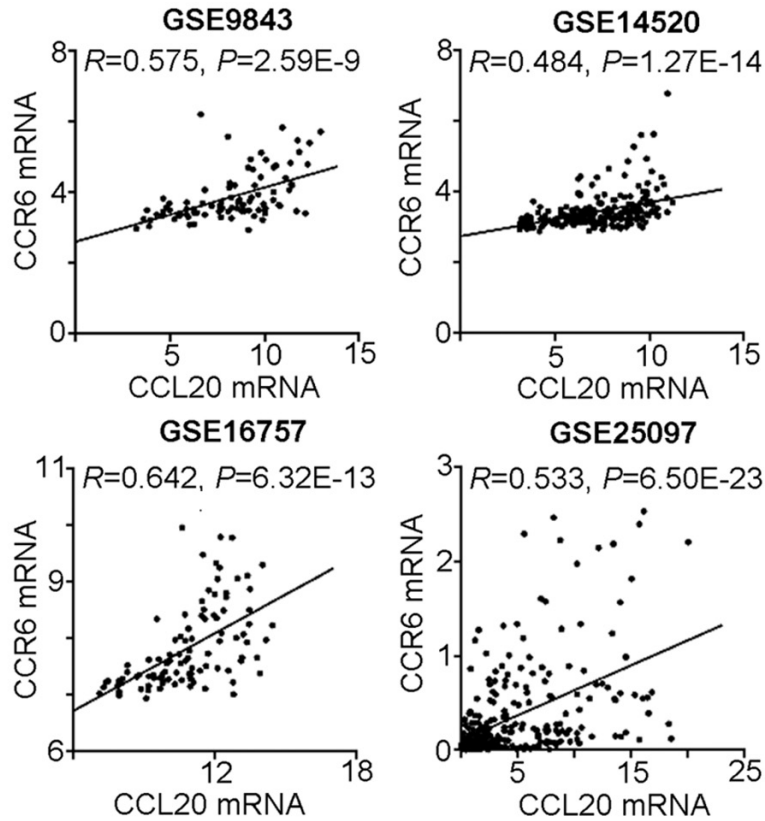


Supplementary Figure 1. Cell viability and Transwell migration array of H22 cells cultured with medium in the presence or absence of anti-CCL20 neutralizing antibodies at indicated time points. A. Cell viability of H22 cells treated with or without anti-CCL20 neutralizing antibodies at selected time points were determined by CCK8. B. The migration potential of H22 cells treated with or without anti-CCL20 neutralizing antibodies were measured by Transwell. Isotype, rat IgG₁; anti-CCL20, anti-CCL20 neutralizing antibody. Data, mean \pm SD.

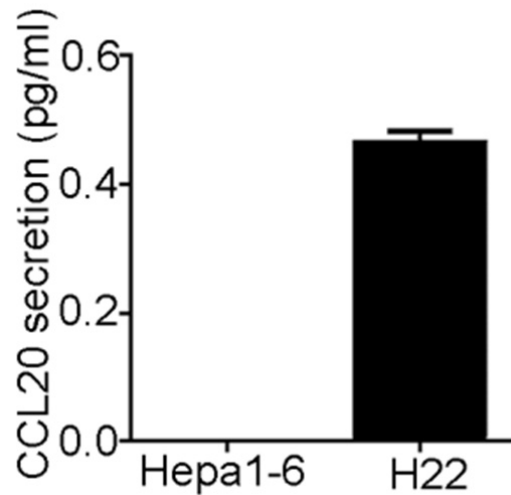


Supplementary Figure 2. The expressions of CCR6 in human HCC cell lines and murine hepatoma cell lines were analyzed by FCM.

CCR6⁺ B lymphocytes recruited by tumor-secreted CCL20 promote HCC progression

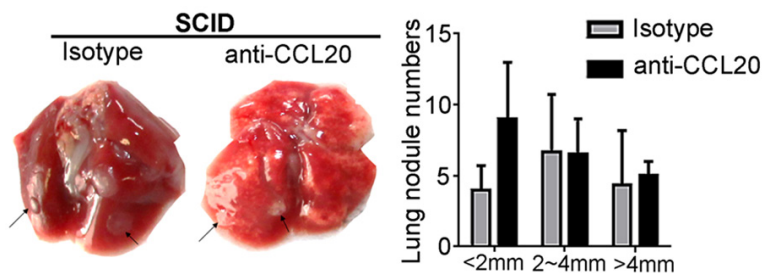


Supplementary Figure 3. The correlation between CCL20 and CCR6 mRNA was analyzed by Pearson's method in HCC patients' tissues from four independent published data sets.

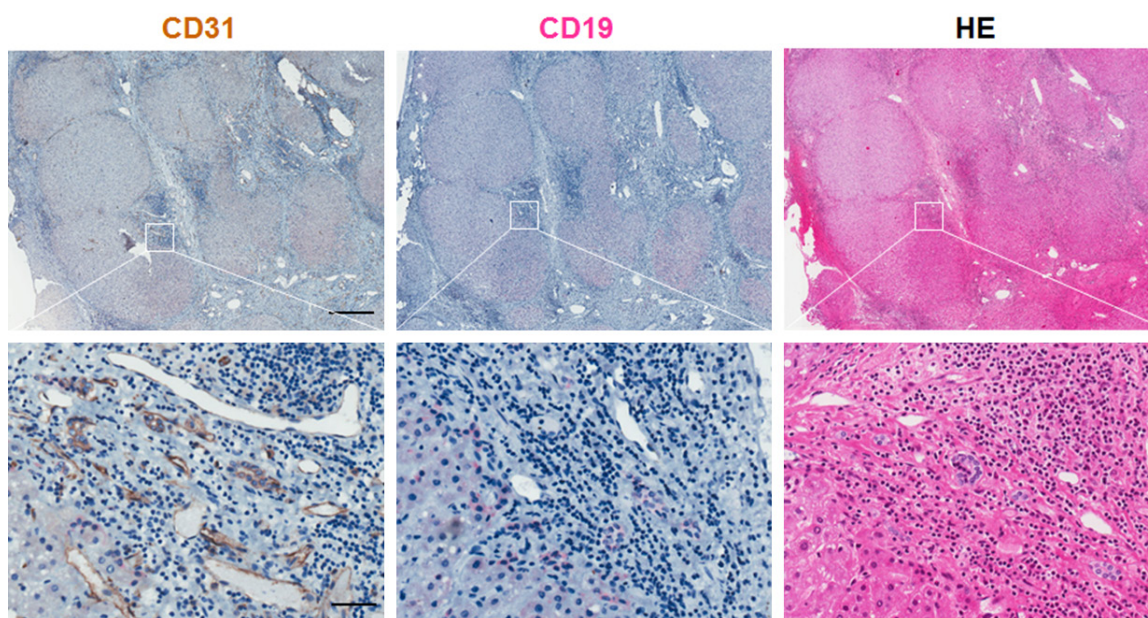


Supplementary Figure 4. CCL20 concentration in the culture medium of Hepa1-6 and H22 cells was assayed by ELISA. Data, mean \pm SD.

CCR6⁺ B lymphocytes recruited by tumor-secreted CCL20 promote HCC progression



Supplementary Figure 5. Representatives of the gross images of lungs isolated from SCID mice that received intravenous injection of 1×10^6 H22 cells in 0.2 ml PBS and treated with 100 μ g anti-CCL20 neutralizing antibodies or rat IgG₁ isotype control twice in the first week after inoculation (left panel). The numbers of metastatic nodules in the lungs (right panel, n=3 for rat IgG₁ isotype control group and n=2 for anti-CCL20 group). Data were presented as mean \pm SEM.



Supplementary Figure 6. IHC showing microvessels (CD31, brown) and B cells (CD19, red) staining in the same HCC samples; scale bars, 500 μ m (upper panel) or 50 μ m (lower panel).